
Thermal Stress Analysis of the SLC Target for Potential Use at the International Linear Collider

DESY Summer Student Programme, 2014

James A. Howarth

Lancaster University, England, United Kingdom

Supervisors

Dr. Sabine Riemann & Dr. Friedrich Staufenbiel



5th of September 2014

Abstract

This report details preliminary results from simulations, testing the viability of the SLC target, for use as a conventional target for the ILC positron source. The results included here focus on both the normal and von Mises stresses in the target, due to the thermal heating that occurs when positrons are produced. The von Mises stress is compared with results from a previous simulation, testing stresses in the SLC target. We note that the normal stresses in the target immediately after heating seem much higher than was previously expected. A few notes are also included referring to issues that may be encountered using ANSYS for similar simulations.

Contents

1	Introduction	3
1.1	The International Linear Collider	3
1.2	Positron Source	4
2	Theory	5
2.1	Normal Stress	6
2.2	von Mises Stress and Yield Criterion	6
3	Method - ANSYS Simulations	6
3.1	Modelling the Energy Deposition	6
3.2	Creating the Target and Mapping the Mesh	7
4	Results and Analysis	8
4.1	Comparisons with Expected Results	8
4.2	Stresses and Spallation	8
4.3	Minor Oscillations	10
5	Conclusions	11
6	Acknowledgments	11
	Bibliography	12

1 Introduction

Particle colliders represent one of the most useful tools currently available for conducting particle physics experiments and are therefore vital for improving our understanding of the universe. Particle colliders have facilitated the discovery of a plethora of new particles, as well as providing invaluable insights into the fundamental processes by which particles interact. With the recent discovery of the Higgs boson, made at the Large Hadron Collider in 2012, it appears as if the standard model may be complete. However, there are still plenty of questions that need to be answered in the field of particle physics. In addition to in depth study of the Higgs, there are many other directions for potential particle physics experiments including: top physics studies; improved precision measurements of particle coefficients and masses; and the search for new physics, beyond the standard model. [1][2]

Currently, the best tool available for performing these experiments is the LHC at CERN, due to the high energies available to it. However, due to the use of protons as the colliding particles in the LHC, it will be difficult to get very precise measurements for any of these experiments. The reason for this is due to composition of a proton. Protons are composite particles, consisting of three valence quarks and a sea of virtual quarks, antiquarks, and gluons. This means that, in any interaction, the reconstruction of the hard scattering process of interest requires great effort. Rather than using protons, it is a much cleaner to use point like particles, such as leptons, as the collision particles, as these are very clearly defined and easier to follow. Lepton collisions also produce a lot fewer unwanted processes, reducing noise in the detector that may have made distinguishing interesting processes difficult. The main weakness of lepton colliders is due to the smaller rest mass of the particles. This means that synchrotron radiation becomes a significant barrier to the achievable energy in any circular collider. As far as lepton colliders are concerned, the majority of designs, both working and conceptual, are electron-positron colliders. If these colliders are to achieve energies similar to or greater than those at the LHC, then they must be linear colliders to remove the issue of synchrotron radiation. [3]

1.1 The International Linear Collider

The International Linear Collider (ILC) is a proposed electron-positron collider, that could be used to find answers to many of the important questions existent in particle physics. A diagram of the most recent design for the ILC, as of writing this report, is shown below in Figure 1. [4]

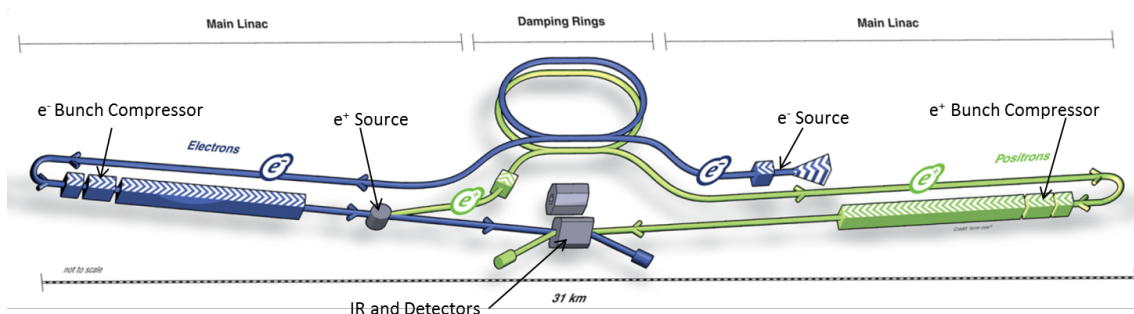


Figure 1: A diagram of the ILC showing the various components. This design is optimised for 500GeV operations. Image adapted from one included in the ILC executive summary. (Courtesy: ILC GDE)[5]

The various sections of the ILC design are shown, simplified, in this diagram.¹ The main linacs are each roughly 11km in length, but will need to be extended if the ILC is to be upgraded to higher energies. Near the start of the main linacs are the bunch compressors, for the positrons and electrons. It is desired that the ILC will be able to achieve far

¹For a detailed description of the ILC please see the ILC technical design reports.

more condensed bunches than any of its predecessors, such as the SLC, which will significantly improve the quality of the results achievable. After the compression stages, the bunches will begin the full acceleration, accelerating the particles from around 15 GeV up to 250 GeV. This shall be achieved by using approximately 7400 superconducting Niobium cavities using RF pulses; typical to many accelerators. There are two possible detectors, of different designs, that may be used for detecting the event. Design work for how to swap these detectors quickly and accurately is also being done at the moment. The purpose of the two detector design is to ensure that the inherent systematic errors, prevalent in each individual detector will not have any influence on the overall results obtained at the ILC. Finally, the central-region also contains the damping rings, as well as the individual sources of the two beams. [4][5][6]

In addition to high energies, it is important that the ILC is capable of producing a high rate of processes, to provide plenty of analysable events. This means it is important to maximise the luminosity of the collider, as well as the cross sections for any reactions. One way to increase the cross section is to polarise the electrons and positrons, prior to the collision event. This must therefore be kept in mind when considering the designs for the two sources. So far it has been decided that the electron source beam shall be produced by a laser illuminating a strained GaAs photocathode. Using this it should be possible to achieve up to 90% polarisation for the electron beam. The final positron source design is still in consideration. [4]

1.2 Positron Source

Unfortunately, polarising the positron source is a more complicated task. Below in Figure 2 is the most recent design for the entire positron source section of the collider. The electron beam produced for collision events is also used to create the positrons at the positron source. The electron beam passes through a helical undulator producing circularly polarised photons. These photons are then incident on the target producing longitudinally polarised positrons which are then separated from the residual electrons and photons using electromagnetic fields. The positrons are then accelerated and transferred to the damping rings before the beginning the main acceleration. [4]

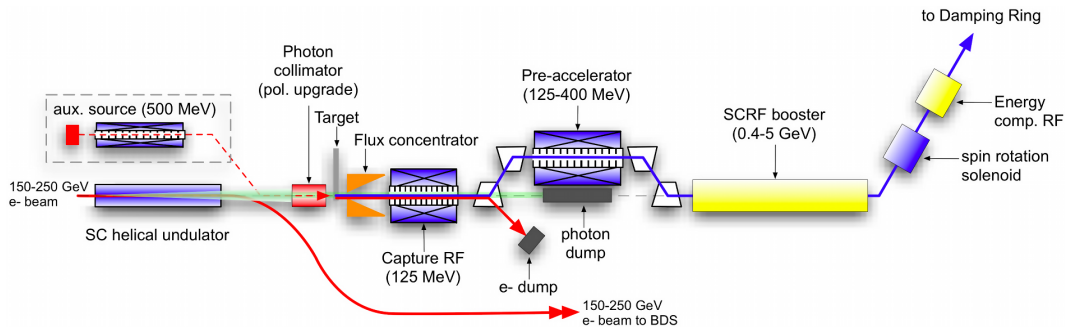


Figure 2: *The current diagram showing the components making up the positron source for the ILC*[4]

There is, however, still some concern with regards to this design; especially whether the positron target is fit for purpose for the ILC. The design should, if successful, be able to produce positrons with a polarisation of 30%, with scope for further upgrades, by collimating the photon beam and extending the undulator, that could achieve 60% positron polarisation. Unfortunately, there remain a number of engineering challenges, specifically with regards to the positron target. Practical experiments at the Lawrence Livermore National Laboratory demonstrated some of the difficulties prevalent in designing a suitable vacuum seal for the target wheel, with the initial ferrofluid prototypes failing far earlier than would have been hoped. In addition, simulations using ANSYS at DESY have shown that further issues may arise due to excessive force in the bearings of the wheel which would also limit the lifetime of the positron source target. A diagram of the target intended is

shown below in Figure 3a. [7][8]

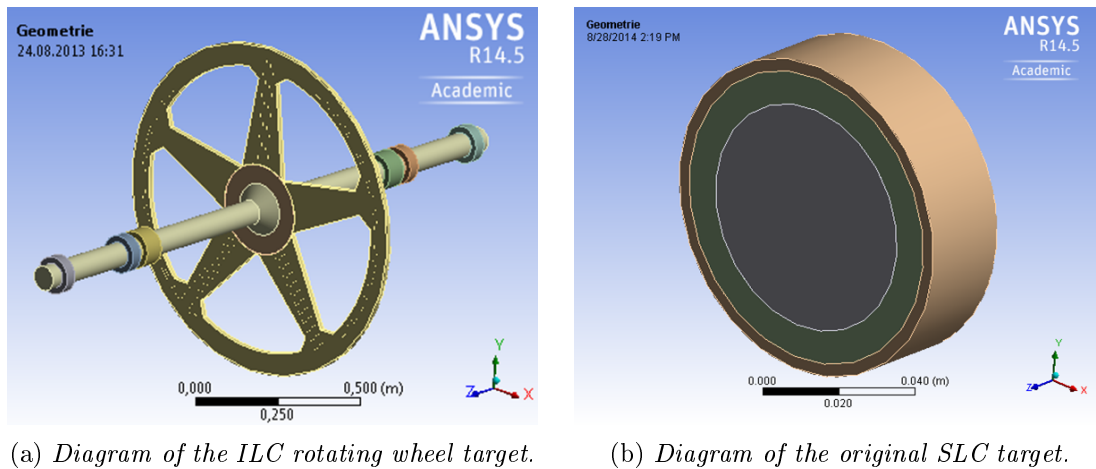


Figure 3: *Two of the many ILC positron target proposals.*

This has led to alternative target suggestions that could produce positrons. While studies continue to be done improving the undulator-based source others focus on testing potential conventional sources. Conventional sources use high-energy electron beams colliding a thick, fixed target to produce an electromagnetic shower. One such conventional source would be to use a design similar to the SLC positron source target, used at the Stanford Linear Collider, shown in Figure 3b. This design appeals to the more conservative elements in the ILC design as it will ensure that the ILC has positrons for collisions. However, a significant drawback to using a conventional target is that they are incapable of producing polarised targets, thus reducing certain capabilities of the ILC. [9][10]

While work is continuing to be performed, attempting to resolve the issues of the, preferred, rotating target wheel (Figure 3a), it is important that simulations are also performed on potential conventional sources, such as the SLC target. By doing such simulations it is possible to ensure that, whatever target design is finally selected, the ILC will have a viable working target for producing positrons. This report details work done performing initial thermomechanical stress tests on an SLC-like target in the hopes of understanding why the original SLC target failed. The SLC target is known to have operated successfully for two years before the target failed due to excessive spallation. [11]

2 Theory

Due to the focus on stress in this report, it is important to give some explanation of what stress is and why it must be considered in the design process. To describe it simply: stress is defined as the average force per unit area exerted by one particle on another across a chosen surface.

$$\sigma_{Stress} = \frac{F}{A} \quad (1)$$

However, there are numerous different types of stress describing the different ways in which a particle exerts forces on those surrounding it. Simple stresses include uniaxial normal stress, shear stress and isotropic stresses. However, to obtain a general stress for a mechanical body, it is often necessary to consider a complex of such stresses, usually described by the use of tensors. This report focuses on both normal stress for relevant planes of interest, and the von-Mises stress and yield criterion. In this context these two stresses are both thermal stresses caused by the temperature gradients formed during positron production. [12]

2.1 Normal Stress

Normal stress is defined by the selection of a plane within or on the material. This plane may be imaginary or an actual surface somewhere on the material. One way of defining a plane is to define it by a unit vector perpendicular to the surface at all points. The normal stress experienced by an object at a point is defined as the stress pointing in a direction parallel (or anti-parallel) to the vector defining the plane. Normal stresses may be defined either for simple situations or as a vector component of the stress tensor, parallel to the standard normal stress vector. [12]

2.2 von Mises Stress and Yield Criterion

The von Mises yield criterion is a plasticity theory describing the point at which a material shall begin to deform plastically and therefore irreversibly. The yield criterion may be formulated in terms of the von Mises stress, or equivalent tensile stress. The von Mises stress is given by the equation:

$$\sigma_{vonMises} = \sqrt{\frac{(\sigma_{11} - \sigma_{22})^2 + (\sigma_{22} - \sigma_{33})^2 + (\sigma_{33} - \sigma_{11})^2 + 6(\sigma_{12}^2 + \sigma_{23}^2 + \sigma_{31}^2)}{2}} \quad (2)$$

Written in terms of the Cauchy stress tensor components σ_{ij} as defined below in Figure 4. According to the von Mises yield criterion, yielding will occur when the von Mises stress exceeds the yield strength of the material in simple tension. [12]

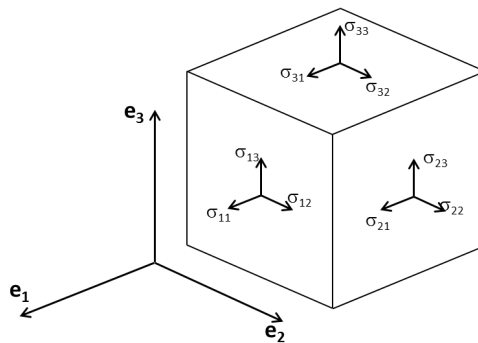


Figure 4: A diagram showing the formalism for the Cauchy stress tensor components.

3 Method - ANSYS Simulations

To fully and accurately simulate the thermal stresses that will be experienced by the SLC target, it was decided to use ANSYS structural analysis software. ANSYS simulation software utilises the finite element method, using variational calculus to minimise error functions at the element boundaries. All simulations currently being performed for ILC positron source targets use the same software, allowing for easy comparisons to be made.

3.1 Modelling the Energy Deposition

The first aim of the work was to recreate and verify the results produced in an earlier paper simulating stresses in the SLC target (W. Stein 2002 [11]). The purpose of this analysis is to, hopefully, understand the reasons why the SLC target eventually failed. By looking at the stresses experienced by the target, and comparing these values to the calculated yield stress of the materials, it is hoped that some insight into the spallation process can be gained. Stein's paper detailed the dimensions and material composition of the SLC target, as well as the details of the energy deposition in the SLC target. The electron beam consists of 4.0×10^{10} electrons/bunch at an energy of 33GeV. This causes a deposit of 5kW of power into the target at a frequency of 120Hz. The beam has a Gaussian radial

distribution and forms a spot of size 0.8mm. Using the details of the energy deposition Dr. Staufenbiel created a heater profile for use in the simulation. [11]

3.2 Creating the Target and Mapping the Mesh

Before the heater profile could be imported onto the target it was necessary to create the target and then map a mesh of suitable standard to obtain the desired detailed analysis. The cooling pipes were removed from the design to reduce the complexity of the simulations. This was deemed an acceptable simplification as the pipes should not significantly influence the main results. In addition it was decided that only one quarter of the circular target needed to be considered to further reduce computation time and power.

The next step, once the target had been created to the specifications, was to map the mesh. The ideal mesh for the settings used would be one consisting entirely of cubic elements, as fine as possible. This must, however, be balanced with certain other constraints to obtain a suitable compromise. One of the most important limiting factors on the capabilities of numerous parts of the simulation is the amount of time available for running the simulation. The more elements that are added, or the more analysis steps and substeps, the longer the simulation will take. This is compounded by another necessary constraint on the simulations: to ensure that the simulation shall give physical results, the longest time period of a step may not exceed the time it would take for sound to travel through the smallest element. This means that all time periods must be smaller than t_{max} as given by:

$$t_{max} = \frac{\text{smallest element length}}{c_s} \quad (3)$$

Where $c_s = 5174ms^{-1}$ for Tungsten. Therefore as the mesh size is reduced it lowers the maximum time step that may be used in calculations. The SLC's beam impinged on the target at a position 2.75cm from the central axis, ensuring all of the beam spot is within the tungsten material. The heater file was imported in the correct position, to correctly simulate the heating and temperature changes in the target. This imported heat is then used to create a temperature profile across the entire target over a desired amount of time. The resulting temperature profile was closely checked afterwards, to ensure that it matched with all desired parameters from W.Stein's report. Figure 5 shows the target with the final mesh mapped onto it and the beam-spot temperature profile imported.

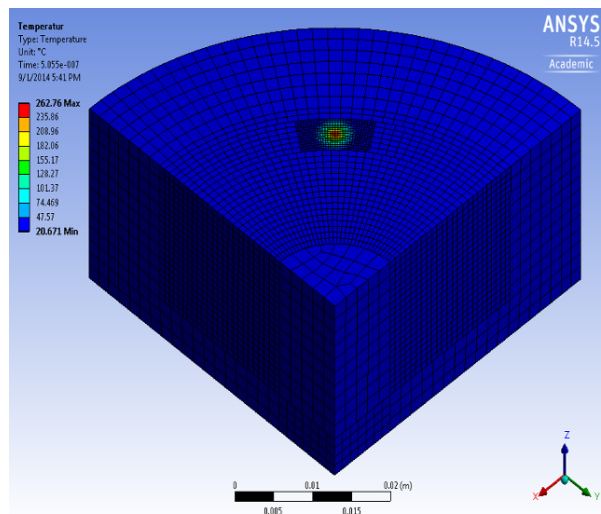


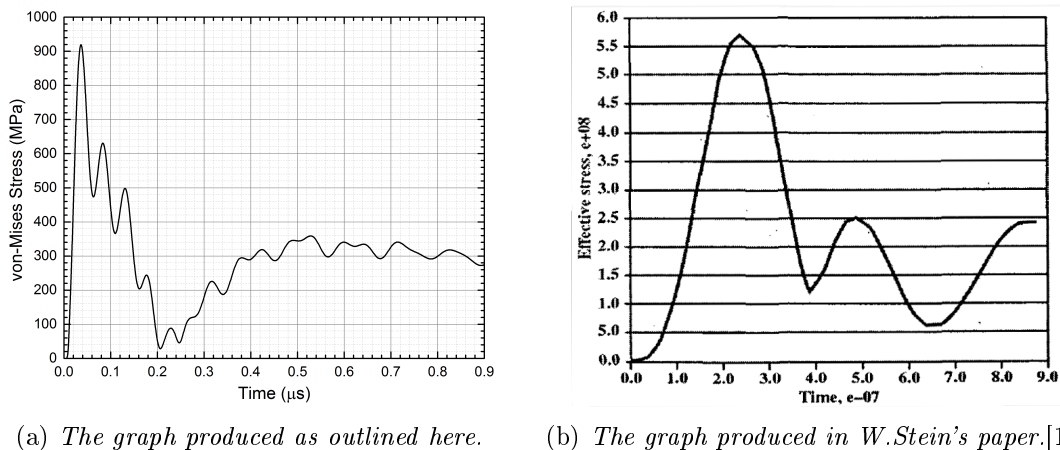
Figure 5: Diagram showing the final mesh used for the results of this report, mapped onto the target. This mesh consists of a total of 56,440 elements, 34,170 of which are located in the most dense region where the beamspot is added.

4 Results and Analysis

Once the temperature had been correctly imported, and shown to be exhibiting physically viable behaviour, it was possible to begin the full simulation, to analyse how the target would behave. In the SLC target, the majority of cracks and spallation occurred at the exit surface for the electron beam. This means, it is of great importance that the stress is fully understood and analysed in these regions. For this reason, one of the main areas of study looked at the various kinds of stress at different depths along the beam's trajectory. To do this, stress probes were placed along the trajectory at intervals of 0.25mm . Not all of these probes were intended for use: many were placed to ensure that nothing unphysical was occurring between the desired measurement points. The results from these probes were then copied into origin to produce graphs.

4.1 Comparisons with Expected Results

Firstly, a graph was created to match the one provided in the W.Stein report. The graph shows the von Mises stress at the exit surface of the SLC target for the first $0.9\mu\text{s}$ of the simulation. This is shown in comparison to the original below in Figures 6a and 6b.



(a) *The graph produced as outlined here.*

(b) *The graph produced in W.Stein's paper.[11]*

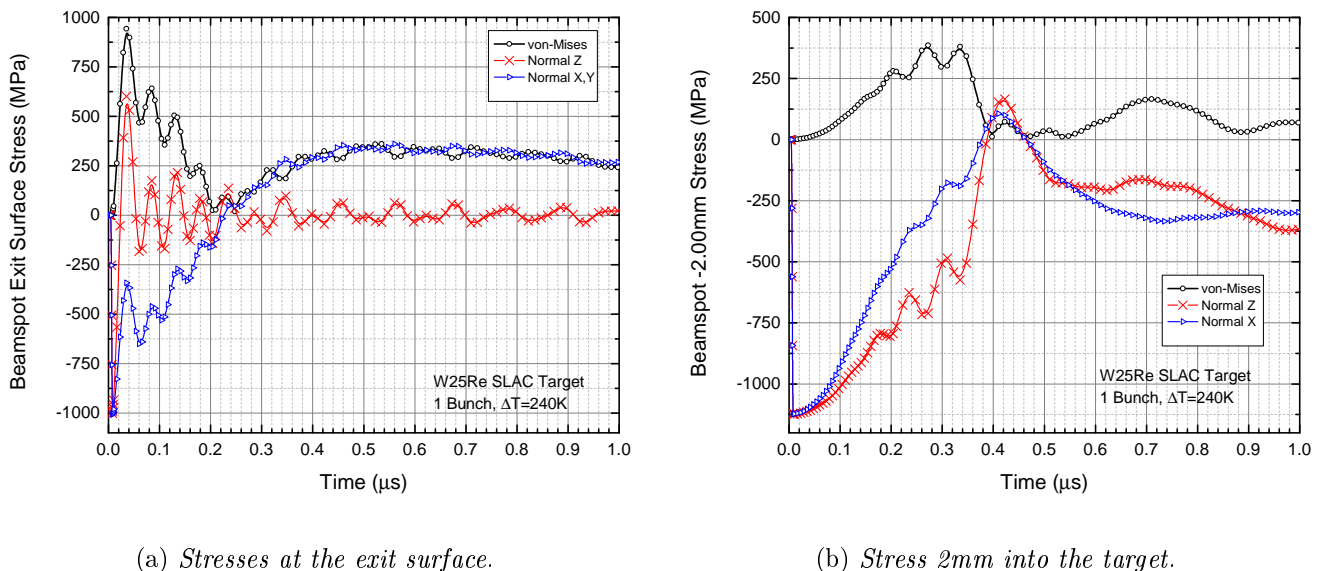
Figure 6: *Two graphs comparing the development of von Mises stress at the exit surface and centre of the beamspot for different simulations.*

It is immediately obvious that the two graphs do not match. The most striking difference is the presence of minor peaks and troughs in the curve produced by my simulations. These shall be discussed later, if they are ignored for now then the curve appears to follow a general curve of similar shape to the curve produced by Stein. However, the peak and trough of this curve are at different points and at different intensities; in fact where Stein's graph reaches a peak we note that the more recent simulation is at its minimum. One of the most plausible reasons for these differences is due to the different choice of time stepping and mesh sizing, between the two simulations. We observed that Stein used a much larger mesh element size and considered that, due to certain features of the graph, the time steps were likely to be larger than those used in our simulations. The software used by Stein is slightly different to that used here, which is likely to introduce some small differences between the two results, though this can not account for everything we see here. To test this theory, a new simulation, with larger mesh elements and longer time steps, was performed. The results from this simulation were much more similar to those presented by Stein. [11]

4.2 Stresses and Spallation

Stein's paper only included one graph, and therefore only one comparable graph could be produced here. However, plenty of other results were produced during my simulations. Unfortunately, only a fraction of this could be included, so I have tried to choose the more interesting pieces. The following graphs, Figures 7a and 7b, show the von Mises stress and

normal stresses existent in the target at two different depths along the beam line. The selection of depths was influenced significantly by results from other simulations looking at other targets. It had been noticed in other simulations, looking at a target design named the 300Hz target, that the maximum von Mises stress was not experienced at the exit surface and instead at a depth $\approx 2\text{mm}$. These simulations were conducted by Felix Dietrich for his bachelor thesis at the University of Wildau. [13]



(a) *Stresses at the exit surface.*

(b) *Stress 2mm into the target.*

Figure 7: *Two graphs showing the von Mises and normal stresses experienced by the target at two different depths.*

It is useful to analyse these graphs both individually and then in comparison with each other. Figure 7a shows that, immediately after heating, though the von Mises stress appears to be zero, the normal stresses in the target have very large values. It is important to understand whether these large values are accurate depictions of the forces felt by the material. In some cases, if a high stress is measured isotropically there may not be any yield as plastic flow does not occur. This appears to be what the von Mises stress value is showing. However, it is unclear at the present time whether this is accurate. If the normal stresses are present and the figures we see are physical then this graph may give a good hint as to why the target failed. The graph also shows the minor oscillations that follow the curve, and how these oscillations reduce as time goes on. [11][14]

The second graph shows the same three different stresses. Again, it is notable that the von Mises stress appears to be approximately zero immediately after heating, while the normal stresses are again very high intensity. This graph is perhaps more interesting, as it takes quite a bit longer for the two stresses to reduce in intensity. Assuming no critical flaws in the simulation as a whole, this would strongly suggest that the normal stresses initially shown are indeed occurring in the material. It is interesting to once again note the minor oscillations. In this case the oscillations do not appear until around $0.2\mu\text{s}$. Comparing the two graphs we note that the von Mises stress appears to have decreased as we go into the material. However, if we instead look at the normal stresses we notice that the absolute value has in fact increased. Perhaps most interesting about this is that the absolute value of this normal stress is in fact largest 2mm into the material, potentially tying in with the results found for the 300Hz target.

The yield stress for the tungsten is quoted in [11] as being between 1.3GPa and 1.6GPa for the temperatures analysed. The normal stress values shown here correspond to ap-

proximately 75% of the material yield stress. This is a very large value: much higher than was expected from previous results. It is now important to establish the accuracy of these values and to determine whether the target material is fully experiencing these stresses. If this can be done then we will be much closer to understanding fully why the SLC target failed and have therefore made additional progress towards realising a practical and legitimate positron source.

4.3 Minor Oscillations

One interesting feature to the graphs shown so far is the minor oscillations that appear to follow the main stress curves. It is unclear, simply from these graphs, whether these oscillations are physically happening or due to some issue with the setup of the simulation. One theory that was proposed was that the oscillations were due to an issue with reflections being caused by the individual elements not lining up cleanly.² To test this, another simulation was performed using the same time-stepping but with a finer mesh in the central region. This provided a new set of results that could be compared with those before, as shown in Figure 8 below.

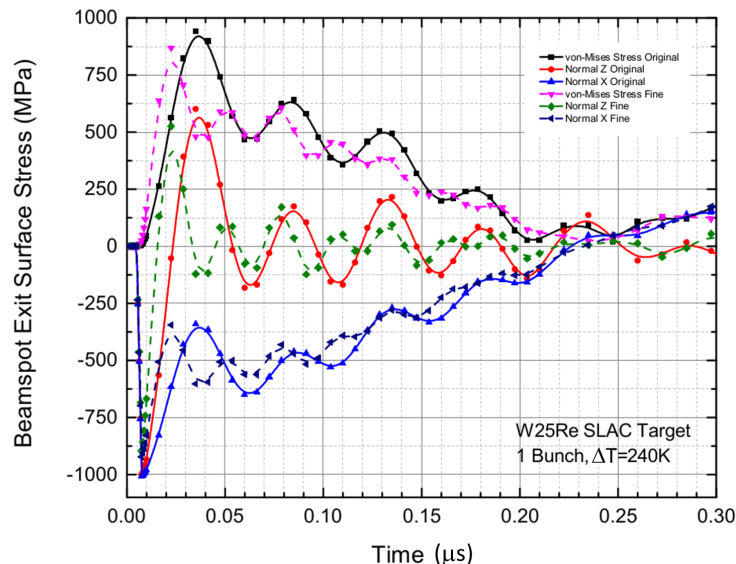


Figure 8: Graph to compare the stresses for two different central mesh sizes.

From this graph the oscillations are shown to have a different period. In the first mesh setup the oscillations produced have a period of $46ns$, while the second mesh produces oscillations with a period of $28ns$. These values do indeed appear to match up with the element size selected for the central region. For the first mesh the elements were roughly $0.3mm$ in each length, corresponding to a minimum time of around $55ns$ for sound to travel across the element. The second mesh size matches even closer, with the elements halved in size to around $0.15mm$ this time corresponding to $29ns$.

Though the stress wave travels in all directions equally, we would not expect to see equally intense reflections from directions that do not intersect elements perpendicularly. This encourages the argument that the oscillations are artificial. One note of consideration is that this does not appear to match with what is shown in Figure 7b. It would be expected that the oscillations in the wave would begin almost immediately, as they do in Figure 7a. It is unclear why this difference occurs. However, it may simply be that the reflections earlier are not as significant and therefore do not show up as clearly in the results. Alternatively, these oscillations may be somewhat physical. It is therefore necessary to check these results carefully.

²Another theory for these is currently being tested, but will not be finished before this report is due

5 Conclusions

This report details a small selection of the results obtained from simulations of the SLC target during positron production. In addition to the stresses down the beam line, it was important to look radially at varying depths to see how the stress wave evolved over time and position. The velocity of particles and deformation of elements was also studied in great detail as other areas of study. Unfortunately, it was not possible to include most of these results while still keeping the document concise. The main physical result of the simulations was the revelation that the normal stresses experienced in the material are much higher than was previously anticipated. Further work will be needed to verify these results fully. In the case that these results are verified, we will have a much better idea why the SLC target failed. This is valuable information that may be used when comparing the strengths and weaknesses of the various targets that could be used in the ILC. If the SLC-like target is chosen, then the results will be invaluable for understanding how best to preserve the target and extend its overall lifetime.

The simulations also demonstrated the significance of selecting a fine mesh and using short time step intervals. Comparing the results produced here with those by Stein, it seems to suggest that significant details are missing from the curve produced by Stein. It is therefore imperative that sufficiently detailed analyses are performed on each target to ensure that no details are missing in the results. In addition, I also noticed some issues with setting up the simulations in ANSYS. The main issue outlined here was the issue of, what we believe to be, artificial oscillations in the curve, most likely caused by reflections off the sides of elements. I have recently been informed that a similar issue was also experienced by the person performing simulations on the 300Hz target before me. In this he discovered that there was in fact a specific way that each mesh had to be set up to ensure that all elements would connect together correctly. Unfortunately, this information was received too late for corrections to be made to my simulations. Hopefully, it will be possible for him to continue from where my work ended, with this correction in mind and eliminate any artificial features.

The simulations outlined here are a good starting point to fully understand the SLC target. Further work must be done both to verify the results obtained here and to investigate further the various stresses and strains within the target. While this report details only the stress results along the beam-line, a number of other measurements were also taken. Firstly measurements were taken looking at how the stress wave propagates through the material, looking at the evolution of time in positions radially equidistant from the beam-spot, at various depths. There were also two entire other sections of the project looking at the velocity of particles in the target and the deformation experienced. These results have not been analysed to the same degree as the stress results and therefore, in the interest of keeping the report concise, were not included here. Once these simulations have been fully completed and verified there are a number of other tests that need to be done for the SLC target. It should be noted that all results included in this report are for the production of only one bunch. The actual positron source target shall be producing many bunches at quite a fast rate and it will be important to perform simulations looking at how the target behaves over an extended period of time.

6 Acknowledgments

I would like to thank a number of people without which this work could not have been produced. Firstly I would like to thank Felix Dietrich and my supervisor Dr. Staufenbiel for their tuition and assistance regarding the use of the ANSYS simulation software. I would also like to thank my supervisor Dr. Riemann for her in depth explanations of the workings of the ILC and for helping me to interpret many of the results I obtained. Finally I would like to thank Karl Jansen for organising the 2014 DESY summer student programme, providing such a brilliant opportunity to gain valuable experience working in physics research.

References

- [1] CMS Collaboration: Chatrchyan, S., et al., “*Observation of a new boson at a mass of 125 GeV with the CMS experiment at the LHC*”, *Physics Letters B*, Volume 716, Issue 1, Pages 30-61, ISSN 0370-2693, <http://dx.doi.org/10.1016/j.physletb.2012.08.021>. 17 September 2012
- [2] ATLAS Collaboration: Aad, G., et al., “*Observation of a new particle in the search for the Standard Model Higgs boson with the ATLAS detector at the LHC*”, *Physics Letters B*, Volume 716, Issue 1, Pages 1-29, ISSN 0370-2693, <http://dx.doi.org/10.1016/j.physletb.2012.08.020>. 17 September 2012
- [3] Griffiths, D. J., “*Introduction to elementary particles*”, Pages 257-276 Wiley, Weinheim, 2008
- [4] Adolphsen, C., et al., “*The International Linear Collider Technical Design Report - Volume 3.II: Baseline Design*”, arXiv:1306.6328 [physics.acc-ph], 26 June 2013
- [5] Behnke, T., et al., “*The International Linear Collider Technical Design Report - Volume 1: Executive Summary*”, arXiv:1306.6327 [physics.acc-ph], 26 June 2013
- [6] Baer, H., et al., “*The International Linear Collider Technical Design Report - Volume 2: Physics*”, arXiv:1306.6352 [hep-ph], 26 June 2013
- [7] Gronberg, J., et al., “*Design and Prototyping of the ILC Positron Target System*”, Talk was presented at the POSIPOL 2014 workshop, Iwate, Japan, 27 August 2014
- [8] Staufenbiel, F., et al., “*Reaction force at the shaft bearings due to imbalances at the ILC target wheel etc.*”, Talk was presented at the POSIPOL 2014 workshop, Iwate, Japan, 27 August 2014
- [9] Seeman, J. T., “*The Stanford Linear Collider*” Stanford Linear Accelerator Center, Stanford University, California, July 1991
- [10] Alley, R., et al., “*The Stanford linear accelerator polarized electron source*” Stanford Linear Accelerator Center, Stanford University, California, 29 March 1995
- [11] Stein, W., et al., “*Thermal Shock Structural Analyses of a Positron Target*”, Proceedings of the Particle Accelerator Conference, 2001. PAC 2001.
- [12] Atkins, A. G., Escudier M. P., “*A Dictionary of Mechanical Engineering*”, Oxford University Press, Oxford, 2013
- [13] Dietrich, F. et al., “*Stress Simulation in the ILC Positron Target with ANSYS*”, Talk was presented at the Americas Workshop on Linear Colliders 2014, Fermilab, Batavia, Illinois, USA, 14 May 2014
- [14] Stephansoson, O., Zang A., “*Stress Field of the Earth’s Crust*”, Chapter 2: *Stress Definition*, Springer, Dordrecht, 2010